Letter

Resonant light enhances phase coherence in a cavity QED simulator of fermionic superfluidity

Shane P. Kelly [1,2,*] James K. Thompson,[3] Ana Maria Rey [2,3,4] and Jamir Marino[1,2]

[1]*Institut für Physik, Johannes Gutenberg Universität Mainz, D-55099 Mainz, Germany*

[2]*Kavli Institute for Theoretical Physics, University of California, Santa Barbara, California 93106-4030, USA*

[3]*JILA, NIST, Department of Physics, University of Colorado, Boulder, Colorado 80309, USA*

[4]*Center for Theory of Quantum Matter, University of Colorado, Boulder, Colorado 80309, USA*

(Received 28 February 2022; accepted 6 October 2022; published 22 November 2022)

Cavity QED experiments are natural hosts for nonequilibrium phases of matter supported by photon-mediated interactions. In this work, we consider a cavity QED simulation of the BCS model of superfluidity, by studying regimes where the cavity photons act as dynamical degrees of freedom instead of mere mediators of the interaction via virtual processes. We find an enhancement of long time coherence following a quench whenever the cavity frequency is tuned into resonance with the atoms. We discuss how this is equivalent to enhancement of non-equilibrium superfluidity and highlight similarities to an analogous phenomena recently studied in solid state quantum optics. We also discuss the conditions for observing this enhanced resonant pairing in experiments by including the effect of photon losses and inhomogeneous coupling in our analysis.

DOI: 10.1103/PhysRevResearch.4.L042032

Superconductivity and superfluidity are among the most celebrated phenomenon of modern condensed matter theory, both for their fundamental importance and for the promise they hold to revolutionize power transmission [1,2]. Recent theory and experimental efforts point at potential nonequilibrium enhancement of superconductinglike phenomena in platforms at the interface of condensed matter and quantum optics, hinting at novel avenues beyond conventional hightemperature superconductors in solid state systems [3–5]. These encompass pump and probe experiments in the solid state setting [6–10], as well as proposals to enhance superconducting order using driven photonic cavities coupled to quantum materials [11–15]. The complexity in modeling the physical principles behind these platforms results from the necessity to combine materials science with an understanding of the role of driven photonic and/or phononic degrees of freedom in many-particle physics [16–33]. It would be therefore desirable to provide an emulator of superconductivity which, although it may simplify the degrees of freedom involved, could shed light on complementary mechanisms for nonequilibrium enhancement of superconducting order. This could then be used as a stepping stone towards richer and more intricate scenarios.

Such an emulator has been proposed in AMO physics for quantum simulation of archetypal s-wave superconductors (for charged particles) or s-wave superfluids (for neutral particles) [34,35]. In these works, the dynamics of the superfluid phase coherence, directly related to the Meissner and Anderson-Higgs mechanisms in superconductors [2], can be studied by monitoring the dynamics of the atomic phase coherence. In the QED simulators considered so far, the cavity must be far detuned from atomic frequencies so that photonic degrees of freedom can be integrated out [36–57] and so an effective matter-only s-wave model of superconductivity is sufficient to describe the dynamics. In such a limit, the cavity only contains virtual photons, and their primary purpose is to mediate pairing interactions.

In this Letter, we investigate the effect of real photons on the phase coherence when the cavity detuning to the atomic transition is reduced. In this limit, the single channel *s*-wave BCS Hamiltonian is no longer an accurate description, and instead the atoms and cavity field simulates the two channel model of the BCS-BEC crossover [2,58]. In this model, the effect of reducing photon detuning on the dynamics are nontrivial because, on one hand, reducing the detuning yields a stronger mediated interaction strength, while on the other hand, reducing the detuning leads to retarded photon dynamics where an instantaneous interaction is no longer valid. Here, we find that even when the change in interaction strength is accounted for, the retarded photon dynamics can maintain phase coherence better than the instantaneous interaction. This is demonstrated in Fig. 1, where we show that upon reducing the photon detuning phase, coherence increases until resonance, below which the diabatic (small detuning) limit takes over and phase coherence is lost. While these results are mostly obtained by a classical integrability analysis [58–65], we also find via numerical simulation that the phenomenon is robust to the nonintegrable effects caused by inhomogeneous couplings and photon loss which are typically present in realistic cavity QED settings.

Simulation of Superfluid Phase Coherence. We consider the simulation of the two-channel model for the BCS-BEC

*shakelly@uni-mainz.de

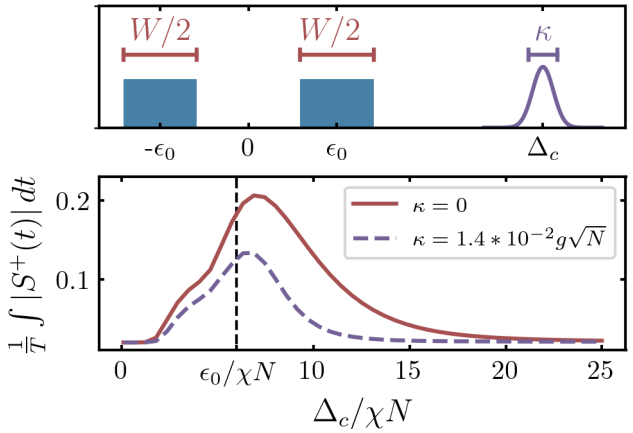

FIG. 1. *Top panel:* A simple schematic of the distribution of atomic levels (see text) and the spectral response of the cavity with detuning Δ_c and linewidth κ. *Bottom panel:* Time average from $t = 0$ to $T = 100/(\chi N)$ of the phase coherence $S^+ = \frac{1}{N}\sum_i \langle \hat{\sigma}_i^+ \rangle$ as a function of the cavity detuning $\Delta_c/(\chi N)$, for large disorder $W/(\chi N) = 8$. In the adiabatic limit, $\Delta_c/(\chi N) \to \infty$, the simulator shows vanishing coherence, $S^+(t) \to 0$, while coherence is maximum when the photon is at resonance with the mean atomic transverse field $\Delta_c \approx \epsilon_0 = 6\chi N$ (marked by a black dashed line). To make use of an integrability analysis, we assume an ideal cavity with $\kappa = 0$ for most of the paper, and then confirm that a realistic cavity linewidth, $\kappa/(g\sqrt{N}) = 1.4 \times 10^{-2}$, does not significantly modify the resonance phenomenon.

crossover observed in ultracold fermion experiments [2,58]. The model involves fermions (with creation operator $\hat{f}^\dagger_{\mathbf{k},s}$ with momentum vector $\mathbf{k}$ and spin s) that can form Cooper pairs on the BCS side of the crossover or bind into diatomic bosonic molecules at zero center of mass momentum (with creation operator $\hat{d}^\dagger$) on the BEC side of the crossover. Neglecting finite momentum molecular bosons, the dynamics are characterized by the Hamiltonian:

$$H_f/\hbar = \sum_{\mathbf{k},s} \epsilon_{|\mathbf{k}|} \hat{f}^\dagger_{\mathbf{k},s} \hat{f}_{\mathbf{k},s} + g \sum_{\mathbf{k}} \hat{f}^\dagger_{\mathbf{k},\uparrow} \hat{f}^\dagger_{-\mathbf{k},\downarrow} \hat{d} + \text{H.c.} + \Delta_c \hat{d}^\dagger \hat{d},$$

where $\hat{d}$ is the mean molecular field, Δ_c is the molecular binding energy, and g is the coupling strength between fermions and molecules. When the fermions condense into a superfluid on the BCS side of the crossover, they mostly form Cooper pairs [2] quantified by the complex pair amplitudes $\rho_{\mathbf{k}} = \langle \hat{f}^\dagger_{\mathbf{k},\uparrow} \hat{f}^\dagger_{-\mathbf{k},\downarrow} \rangle$. In this Letter, we focus on the dynamics of the superfluid s-wave phase coherence $S^+ = \frac{1}{N}\sum_{\mathbf{k}} \rho_{\mathbf{k}}$, which quantifies the phase coherence between Cooper pairs with different pairing wave vector $\mathbf{k}$.

Similar to Ref. [35], the Cooper pairs can be simulated by a collection of two level atoms (described by Pauli operators $\hat{\sigma}_i^+$ and $\hat{\sigma}_i^z$) via the Anderson pseud ospin mapping [58,61,62]:

$$\hat{\sigma}_i^+ \to \hat{f}^\dagger_{\mathbf{k}_i,\uparrow} \hat{f}^\dagger_{-\mathbf{k}_i,\downarrow}, \quad \hat{\sigma}_i^z \to \hat{f}^\dagger_{\mathbf{k}_i,\uparrow} \hat{f}_{\mathbf{k}_i,\uparrow} + \hat{f}^\dagger_{-\mathbf{k}_i,\downarrow} \hat{f}_{-\mathbf{k}_i,\downarrow} - 1, \quad (1)$$

where each atom i simulates a pair of fermion momentum modes $i \to \pm\mathbf{k}_i$. The above Hamiltonian can then be simulated by a cavity QED system similar to the experiments described in references [39,40,42,66], in which the internal levels of $2N$ atoms are encoded in long lived electronic states, e.g., the $^1S_0$-$^3P_1$ states of ^{88}Sr atoms. The atoms are trapped in an optical lattice and are allowed to interact with a single cavity mode (described by a photon annihilation operator $\hat{a}$ simulating the molecular field, $\hat{a} \to \hat{d}$). Such a system is modeled by the Hamiltonian [35,39,40]:

$$H/\hbar = \sum_{i=1}^{2N} \epsilon_i \hat{\sigma}_i^z + \sum_{i=1}^{2N} g_i (\hat{\sigma}_i^+ \hat{a} + \text{H.c.}) + \Delta_c \hat{a}^\dagger \hat{a}, \quad (2)$$

where Δ_c is the detuning of the cavity from the mean atomic frequency, $2g_i$ is the single-photon Rabi frequency, and ϵ_i is an inhomogeneous effective transverse field. Simulation of H_f by the cavity QED system occurs for homogenous light-matter coupling $g_i = g$ and for a probability distribution, $p(\epsilon_i)$, of the inhomogeneous field, ϵ_i, that is designed to match the density of states for the fermion model. We choose the density of states as $p(\epsilon_i) = [B(W/2, \epsilon_0/2, \epsilon_i) + B(W/2, -\epsilon_0/2, \epsilon_i)]/2$, where $B(\alpha, x_0, x)$ is a box distribution with mean x_0 and width α (see Fig. 1). Similar to Ref. [35], such a bimodal distribution is chosen to ensure the possibility of persistent oscillations of the phase coherence (see below) in the $W = 0$ limit. When the disorder strength of the inhomogeneities is not too large $W/2 < \epsilon_0$, the corresponding density of states is associated to a two band model with constant density of states within each band. In [67] we show an example band structure and discuss the superfluid phenomenon that would occur in the traditional thermal equilibrium setting.

At large detuning, $\Delta_c \gg g\sqrt{N}$ and $\Delta_c \gg \epsilon_0 + W/2$, the cavity field mediates spin-exchange interactions and an effective spin model can be derived which maps into a one channel BCS model as discussed in Ref. [35]. In this limit, an adiabatic approximation [35,39,40] assumes the state of the light field is in instantaneous equilibrium such that $\langle \hat{a}^\dagger_{eq}(t) \rangle = -\frac{gN}{\Delta_c} S^+$, where $S^+ = \frac{1}{N}\sum_i \langle \sigma_i^+ \rangle = \frac{1}{N}\sum_{\mathbf{k}} \rho_{\mathbf{k}}$ is both the atomic phase coherence and the simulated superfluid phase coherence. Thus, in the large detuning limit, the photon directly measures the phase coherence S^+. Inserting $\langle \hat{a}^\dagger_{eq}(t) \rangle$ back into Eq. (2) and taking homogenous couplings, one finds a mediated interaction $-\chi \sum_{ii'} \hat{\sigma}_i^+ \hat{\sigma}_{i'}^-$ with interaction strength $\chi = g^2/\Delta_c$ and sign which favors effective Cooper pair formation at low temperatures and positive detuning, Δ_c. In this work we will study the dynamics when the photon detuning, Δ_c, is decreased and the adiabatic approximation is no longer valid. One complication to this limit is that when the photon detuning is decreased, the interaction strength χ increases. To isolate this effect we imagine that the experiment tunes the external magnetic fields controlling ϵ_0 and W such that $\epsilon_0/\chi N$ and $W/\chi N$ are held constant as the photon detuning is decreased. Such an adjustment can be done for separate realizations of the experiment and does not require dynamical control of the external fields during the course of a single experimental run.

Dynamical Phases from classical integrability. To study the dynamics of this system, we make a mean field approximation (i.e., $\langle \hat{O}_1(t)\hat{O}_2(t) \rangle = \langle \hat{O}_1(t) \rangle \langle \hat{O}_2(t) \rangle$ and adopt the notation: $\langle \hat{O}_1 \rangle \equiv O_1$) which is expected to work up to time scales $O(1/(\chi N))$ [68–70]. The resulting classical dynamics of the Hamiltonian in Eq. (2) show Richardson Gaudin integrability [58–65,71,72] in the homogenous limit, $g_k = g$. The so called

Lax integrability analysis [58–65] is then used to study the integrable tori of the classical mean field Hamiltonian corresponding to Eq. (2) and to construct a dynamical phase diagram [35,58] characterizing the collective modes. This is done by studying the conserved quantities to identify a minimum number, M, of collective degrees of freedom (DOF) required to effectively reproduce the dynamics of collective variables at long times [73].

The dynamical phases are then classified by the required number of collective DOF and the dynamics of the phase coherence S^+. First, we consider the resulting collective modes for a quench starting from an initial state with all spins polarized in the $\hat{x}$ direction, $\langle\hat{\sigma}_i^x\rangle = 1$, and the cavity in the vacuum, $\langle a\rangle = 0$. In the spin-only model, three phases are found [35,58] with at most $M = 2$. In contrast, we identify a fourth phase with $M = 3$ upon introducing the photon away from adiabatic elimination. The three phases in the adiabatic limit, $\Delta_c \to \infty$, are (for fixed χN and $\epsilon_0 > \chi N$):

1. *Phase I* ($M = 0$): At large disorder, all phase coherence is lost and the simulated superfluid enters a normal state: $S^+(t) \to 0$.

2. *Phase II* ($M = 1$): Transition to this phase occurs as disorder is reduced, and involves only one effective degree of freedom ($M = 1$). In this phase, the magnitude of the phase coherence, $|S^+(t)|$, is constant at late time, and the collective mode corresponds to precession of the phase of S^+: $S^+(t) \to |S^+|e^{i\mu t}$.

3. *Phase III* ($M = 2$): This phase occurs at even smaller inhomogeneous atomic broadening, and has $M = 2$ DOF. The collective mode shows persistent oscillations in $|S^+(t)|$ as shown in the upper left panel of Fig. 2.

In this adiabatic limit, the critical disorder strength, W_I, between phase I and II, and the critical disorder strength W_{II} between II and III are different $W_I > W_{II}$, and while they depend nontrivially on ϵ_0, they occur on the order of the interaction strength $W_{I(II)} \approx O(\chi N)$. They also depend on the initial state in a nontrivial way [35,58].

At finite detuning, Δ_c, the photon becomes another DOF in the collective oscillations of these three phases, and to distinguish the phases of the full model we will write them with a "+1" superscript. The phases I^{+1} and II^{+1} show the same qualitative dynamics of $S^+(t)$ as the phases II and III, respectively, while a new phase III^{+1} is defined by aperiodic oscillations of $|S^+(t)|$ and requires $M = 3$ collective DOF (two macroscopically coherent spins and a photon). We show an example of these aperiodic oscillations in the top right panel of Fig. 2, where in contrast to phase III, the spectrum contains multiple incommensurate, generally irrational, frequencies which create aperiodic oscillations in the real time evolution of $|S^+(t)|$. As the detuning increases, the aperiodic contribution to the oscillations of S^+ becomes small smoothly as function of Δ_c, and in the large detuning limit, phase III^{+1} approximates phase III. At large but finite Δ_c, the new phase III^{+1} involves the photon performing fast oscillations around $a_{eq}(t)$, the slowly evolving equilibrium value given by adiabatic elimination (see Fig. 2 for an example). In that figure, these extra oscillations have an amplitude $A = \max_t |a(t) - a_{eq}(t)|$ which decreases as $\sqrt{\chi N/\Delta_c}$ with increasing detuning Δ_c, as discussed below. The limiting behavior of the photon dynamics is similar for phases I^{+1} and II^{+1}, and will

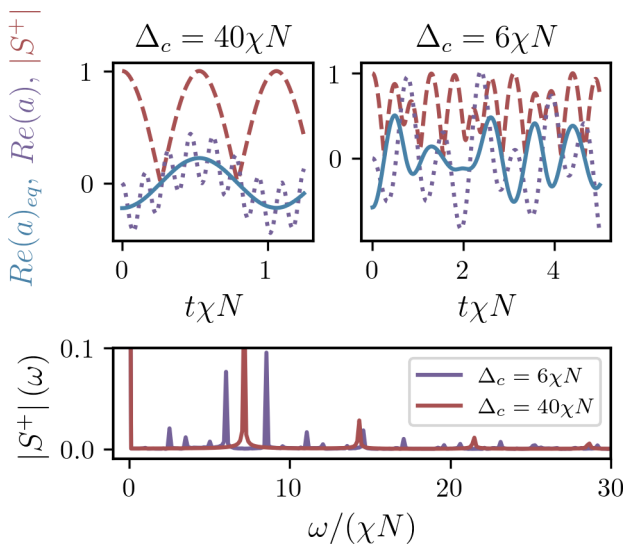

FIG. 2. Dynamics in the homogenous limit, $W = 0$, in both the adiabatic, $\Delta_c = 40\chi N$, and resonant $\Delta_c = \epsilon_0 = 6\chi N$ limits. In the adiabatic limit, the adiabatic approximation correctly predicts the dynamics of the matter, but misses the extra oscillation around $a_{eq}(t)$ predicted by the Lax analysis. While on resonance, the adiabatic approximation is completely wrong and the dynamics of $|S^+|$ show aperiodic dynamics characteristic of phase III^{+1} for any $W \geqslant 0$. The Fourier spectrum, $|S^+|(\omega)$, also shows the difference between the aperiodic dynamics (multiple incommensurate, generally irrational, frequencies) characteristic of phase III^{+1} and the periodic dynamics (one frequency and its harmonics) characteristic of phase III (adiabatic limit of phase III^{+1}).

therefore, at large detuning, ensure these dynamical phases approximate their adiabatic counter parts, phase I and II, respectively.

Upon reducing the detuning, a rich dynamical phase diagram emerges as shown in the upper panel of Fig 3. In that figure we fix $\epsilon_0 = 6\chi N$ such that $W/2 < \epsilon_0$ and the density of state always corresponds to a model with a two band structure [67]. In the $W = 0$ limit, there is only phase III^{+1}, while, at finite W, the cavity field has a broad impact on the dynamical phase diagram. In the diabatic limit, $\Delta_c/\chi N \ll 1$, the dynamics are much more sensitive to the inhomogeneities due to an inability of the cavity to mediate an effective interaction, and the transition to phase I^{+1} occurs at much smaller disorder in comparison to the large detuning limit. We also find a region at large disorder, $W > 4\chi N$, where phase II^{+1} occurs when $\Delta_c \sim \epsilon_0$ which suggests phase coherence can be enhanced by setting the detuning on resonance with the atoms that have atomic energies close to ϵ_0.

Mechanism of resonant phase coherence. The enhancement of phase coherence is confirmed as a function of Δ_c in Fig. 1 for $\epsilon_0 = 6\chi N$ and $W = 8\chi N$, and we explain the formation of this resonance by first considering finite but large detuning, such that $1/\Delta_c$ is still the fastest timescale. In this limit the dynamics are in Phase I^{+1} and the enhancement of phase coherence is very weak at long times, but the following simple picture holds. First, on a timescale of $1/\Delta_c$, the initial polarization of the spins drive the photon into an excited state oscillating around a nonzero $a_{eq}(t = 0) =$

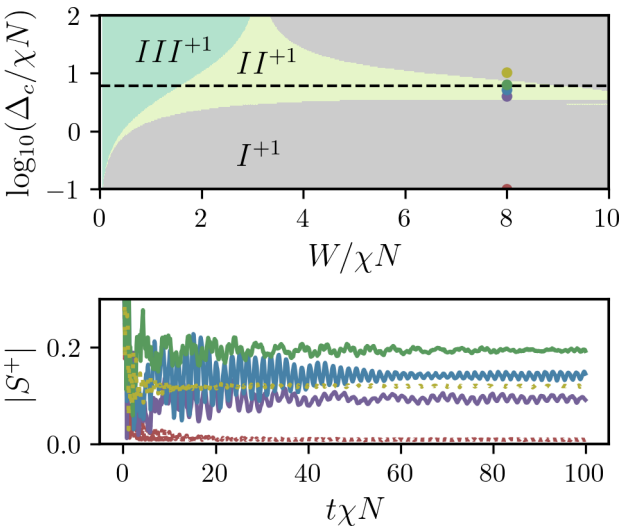

FIG. 3. *Top panel:* Dynamical phase diagram as a function of the cavity detuning and atomic disorder. The approximate resonance condition, $\Delta_c \approx \epsilon_0 = 6\chi N$, is marked by a black dashed line. *Bottom panel:* Dynamics of $|S^+(t)|$ for $W/(\chi N) = 8$ and different values of $\Delta_c/(\chi N)$ as marked by the points in the top panel. For $\Delta_c/(\chi N) = 0.1$ (red) and 10.3 (yellow), $|S^+(t)|$ evolves to a constant steady state characteristic of phase I^{+1}, while for the remaining values of $\Delta_c/(\chi N)$, the dynamics have persistent oscillation characteristics of phase II^{+1}. In this figure, the initial state has $\langle \hat{\sigma}_i^x \rangle = 1$ and $\langle a \rangle = 0$.

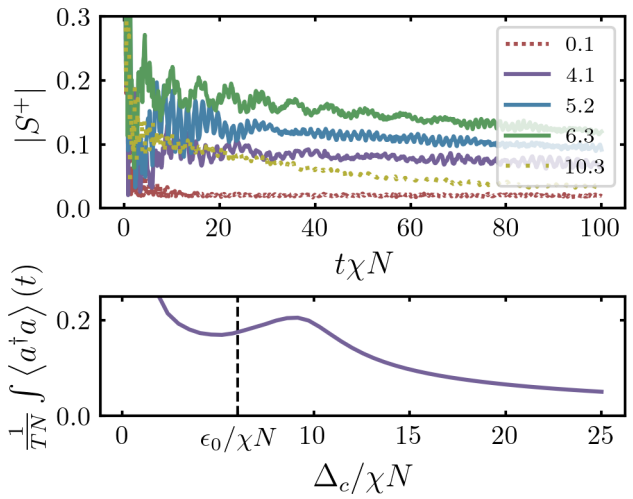

FIG. 4. *Top panel:* Same dynamics for $|S^+(t)|$ as in Fig. 3, but with $\kappa/(2\pi) = 150\,\text{kHz}$ and $g/(2\pi) = 10.8\,\text{kHz}$ as in the experiments of [39,40]. *Bottom panel:* Cavity emission versus detuning Δ_c. This panel is computed assuming inhomogeneous couplings and an initial state prepared by a coherent drive through the cavity. Even though inhomogeneities and cavity losses reduce the coherence, we can observe a signature of the resonance as a minimum [74] in the photon density. Note that in contrast to Fig. 3 and Fig. 1, the initial state depends on the initial number of photons driven into the cavity which scales as $1/\Delta_c$. Both figures were obtained by numerical simulation of the Lindblad equations of motion at mean-field. In the top panel, the decay rate of $|S^+(t)|$ is constant with $\Delta_c/\chi N$ and proportional to $1/\kappa$, but appears to increase with $\Delta_c/\chi N$ in the figure because the unit for time, $1/\chi N$, decreases with Δ_c when g is fixed.

$-Ng/\Delta_c$. Then, on a timescale of $1/W \gtrsim 1/\Delta_c$, the spins mostly dephase and $a_{eq}(t \to \infty) \approx 0$. Once the spins mostly depolarize to their steady state, the photon remains oscillating around a small equilibrium, $a(t) \approx Ae^{i\mu t}$. The Lax analysis (see [58] and [73]) yields expressions for the frequency and amplitude of these small oscillations which have a simple analytical form when $\Delta_c > W > \epsilon_0$: $\mu = \Delta_c$ and $A = \chi N/g = \sqrt{N}\sqrt{\chi N/\Delta_c}$.

From the perspective of the matter, the photon is effectively an external drive that pumps a small fraction of the spins into a coherent steady state. In the frame of reference of the photon (the effective external drive), the dynamics of each spin is fully described by a constant magnetic field, $\vec{h} = (\epsilon_i - \mu)\hat{z} + gA\hat{x}$, and we can solve for the steady state as:

$$S^+ = \frac{1}{N}\sum_i \frac{gA}{\sqrt{(\epsilon_i - \mu)^2 + |gA|^2}}. \tag{3}$$

Since $\mu \sim \Delta_c$, this expression correctly predicts the loss of coherence, S^+, in the adiabatic limit shown in Fig. 1.

Further away from the adiabatic limit, the separation of time scales, $1/W \gtrsim 1/\Delta_c$, that yield the simple picture above is no longer valid. Regardless, the Lax analysis still produces the same expression, Eq. (3), for the phase coherence in phase I^{+1} but now with a different A and μ that must be numerically determined by solving for the roots of a Lax vector (see [58] and Supplemental Material [67]). Since μ gives the precession frequency of the photon, it is expected to be close to the detuning $\mu \approx \Delta_c$ and this is what we find numerically. Equation (3) therefore predicts the atom at site i will be in resonance when $\Delta_c = \epsilon_i$. The coherence is then maximally enhanced when most spins are driven close to resonance and occurs when the drive, Δ_c, is at the center of the band of atomic frequencies $\Delta_c \approx \epsilon_0$. This approximation is confirmed by the peak in coherence shown in Fig 1.

Although Eq. (3) provides an intuitive picture, similar to a single particle resonance, when the system is in phase I^{+1}, the relevant enhancement of coherence at the resonance happens in phase II^{+1} where the cavity field and atomic coherence must both be treated as dynamical variables. As shown in Fig. 3, their dynamics in this regime show coupled nonlinear oscillations [58].

Experimental Realization. In the experiments of Refs. [39,40] an optical lattice is used to trap Sr atoms, featuring a long-lived electronic clock transition with atomic decay rate of γ. The optical lattice is placed inside a standing wave optical cavity with linewidth κ. While both γ and κ destroy phase coherence at long times, we find that the effect of resonant phase coherence is still observable on times $O(1/\kappa)$ provided we operate at large collective cooperativity ($Ng^2 \gg \kappa\gamma$). Given that for long-lived Sr atoms, $\kappa \gg \gamma$ we neglect atomic decay. Figure 1 shows the dependence of $|S^+(t)|$ on Δ_c, and demonstrates that the resonant enhancement can be maintained even with cavity loss. Furthermore, Fig. 4 depicts how the dynamics in Fig. 3 simply features a slow decay for moderate κ.

The experiments in [39,40] also have inhomogeneous couplings $g_i = g\cos(k_0 a_0 i)$ with $k_0 a_0 = 3.7$ due to an incommensurability between the optical lattice spacing, a_0,

and the cavity wavelength, $2\pi/k_0$. The inhomogeneous couplings will disrupt the effect discussed in this work if we start in a homogenous state, since the couplings will no longer excite the photon. However, as long as the initial state is generated by coherently driving the optical cavity, inhomogeneities do not play a detrimental effect. In this case, the initial state involves all spins aligned with the inhomogeneities $\mathrm{sgn}(\sigma_i^x) = \mathrm{sgn}(g_i)$ such that cavity will be coherently pumped by the atoms. The resulting simulations show a signature of resonant phase coherence as a minimum [75] of the time averaged photon density shown in Fig. 4. Note that both dissipation and inhomogeneities break Lax integrability.

Conclusion. Our work demonstrates that dynamical fluctuations of a mediating field can produce enhancement of phase coherence in cavity QED simulators of superconductivity and superfluidity. According to our predictions, the superfluid phase would be quickly destroyed at large detuning, while for resonant detuning the phase coherence of the superfluid would be maintained at long times. It is also interesting to notice that, in addition to phases I, II, and III discussed in Ref. [58], we find the additional phase III^{+1} characterized by long time aperiodic oscillations. This new phase and the resonance phenomenon are allowed to appear, as compared with their absence in previous works [58,61,63], because of a few key differences. One is that the authors in those works did not directly study the question of the effect of the detuning of the cavity, Δ_c, or equivalently the binding energy of the bosonic model, and thus were unable to detect the resonance phenomenon. Another is that we preform a quench from the ground state of a BCS Hamiltonian with no band dispersion and large detuning Δ_c, such that the initial state has zero population of the bosonic mode and a Cooper pair in every accessible fermion mode such that the condensate pairing amplitude is maximal. Finally, in contrast to previous works, our post quench Hamiltonian has a dispersion with two bands. Although these conditions are amenable to prepare in a cavity QED setting, it will be interesting to determine how stringent such conditions are and if similar ones can be prepared to allow the observation of enhanced superfluidity or phase III^{+1} in experiments with superfluid fermions.

Searching for similar physics predicted here in natural extensions of our cavity QED simulator, such as trapped ions or quantum optics in waveguides, both of which serve as tunable simulators of nonequilibrium quantum many body physics, employing mediating photons or phonons [76,77] will be also of great interest. It would also be particularly exciting to search for enhanced superconductivity by a resonant cavity in the charged superfluids of real materials in which the light-matter couplings are structurally different from the atom-molecule couplings of Eq. 1. Overall, our results offer the possibility of studying novel regimes of enhanced cooperative lightmatter, and hint that quantum many-body optics with active light and matter degrees of freedom has the potential to become a blossoming area of quantum simulation in the near future.

Acknowledgments. This work has been funded by the Deutsche Forschungsgemeinschaft (DFG, German Research Foundation) - TRR 288 - 422213477 (project B09), TRR 306 QuCoLiMa ("Quantum Cooperativity of Light and Matter"), Project-ID 429529648 (project D04) and in part by the National Science Foundation under Grant No. NSF PHY-1748958 (KITP program 'Non-Equilibrium Universality: From Classical to Quantum and Back'). A.M.R. acknowledges ARO (Army Research Office) under the Grant No. W911NF-19-1-0210, and the National Science Foundation under the Grants No. NSF PHY1820885. Both A.M.R and J.K.T acknowledge NSF JILA-PFC PHY-1734006, QLCI-OMA -2016244, the U.S. Department of Energy, Office of Science, National Quantum Information Science Research Centers Quantum Systems Accelerator, and NIST.

[1] N. W. Ashcroft, N. D. Mermin *et al.*, *Solid State Physics* (Holt, Rinehart and Winston, New York, 1976).

[2] J. F. Annett, *Superconductivity, Superfluids and Condensates*, Oxford Master Series in Physics (Oxford University Press, Oxford, New York, 2004).

[3] C. M. Varma, P. B. Littlewood, S. Schmitt-Rink, E. Abrahams, and A. E. Ruckenstein, Phenomenology of the Normal State of Cu-O High-Temperature Superconductors, Phys. Rev. Lett. **63**, 1996 (1989).

[4] D. M. Ginsberg, *Physical properties of high temperature superconductors I* (World scientific, 1998).

[5] E. Dagotto, Correlated electrons in high-temperature superconductors, Rev. Mod. Phys. **66**, 763 (1994).

[6] R. Matsunaga, Y. I. Hamada, K. Makise, Y. Uzawa, H. Terai, Z. Wang, and R. Shimano, Higgs Amplitude Mode in the BCS Superconductors $Nb_{1-x}Ti_xN$ Induced by Terahertz Pulse Excitation, Phys. Rev. Lett. **111**, 057002 (2013).

[7] R. Matsunaga, N. Tsuji, H. Fujita, A. Sugioka, K. Makise, Y. Uzawa, H. Terai, Z. Wang, H. Aoki, and R. Shimano, Light-induced collective pseudospin precession resonating with higgs mode in a superconductor, Science **345**, 1145 (2014).

[8] R. Mankowsky, A. Subedi, M. Först, S. O. Mariager, M. Chollet, H. T. Lemke, J. S. Robinson, J. M. Glownia, M. P. Minitti, A. Frano *et al.*, Nonlinear lattice dynamics as a basis for enhanced superconductivity in YBa2Cu3O6.5, Nature (London) **516**, 71 (2014).

[9] M. Mitrano, A. Cantaluppi, D. Nicoletti, S. Kaiser, A. Perucchi, S. Lupi, P. Di Pietro, D. Pontiroli, M. Riccò, S. R. Clark *et al.*, Possible light-induced superconductivity in K3C60 at high temperature, Nature (London) **530**, 461 (2016).

[10] K. Isoyama, N. Yoshikawa, K. Katsumi, J. Wong, N. Shikama, Y. Sakishita, F. Nabeshima, A. Maeda, and R. Shimano, Light-induced enhancement of superconductivity in iron-based superconductor FeSe0.5Te0.5, Commun. Phys. **4**, 160 (2021).

[11] J. B. Curtis, Z. M. Raines, A. A. Allocca, M. Hafezi, and V. M. Galitski, Cavity Quantum Eliashberg Enhancement of Superconductivity, Phys. Rev. Lett. **122**, 167002 (2019).

[12] F. Schlawin and D. Jaksch, Cavity-Mediated Unconventional Pairing in Ultracold Fermionic Atoms, Phys. Rev. Lett. **123**, 133601 (2019).

[13] A. Chakraborty and F. Piazza, Long-Range Photon Fluctuations Enhance Photon-Mediated Electron Pairing and Superconductivity, Phys. Rev. Lett. **127**, 177002 (2021).

[14] M. A. Sentef, M. Ruggenthaler, and A. Rubio, Cavity quantum-electrodynamical polaritonically enhanced electron-phonon coupling and its influence on superconductivity, Sci. Adv. **4**, eaau6969 (2018).

[15] A. Thomas, E. Devaux, K. Nagarajan, T. Chervy, M. Seidel, D. Hagenmüller, S. Schütz, J. Schachenmayer, C. Genet, G. Pupillo *et al.*, Exploring superconductivity under strong coupling with the vacuum electromagnetic field, arXiv:1911.01459.

[16] F. P. Laussy, A. V. Kavokin, and I. A. Shelykh, Exciton-Polariton Mediated Superconductivity, Phys. Rev. Lett. **104**, 106402 (2010).

[17] O. Cotleţ, S. Zeytinoglu, M. Sigrist, E. Demler, and A. Imamoglu, Superconductivity and other collective phenomena in a hybrid bose-fermi mixture formed by a polariton condensate and an electron system in two dimensions, Phys. Rev. B **93**, 054510 (2016).

[18] S. Smolka, W. Wuester, F. Haupt, S. Faelt, W. Wegscheider, and A. Imamoglu, Cavity quantum electrodynamics with many-body states of a two-dimensional electron gas, Science **346**, 332 (2014).

[19] G. Mazza and A. Georges, Superradiant Quantum Materials, Phys. Rev. Lett. **122**, 017401 (2019).

[20] G. M. Andolina, F. M. D. Pellegrino, V. Giovannetti, A. H. MacDonald, and M. Polini, Cavity quantum electrodynamics of strongly correlated electron systems: A no-go theorem for photon condensation, Phys. Rev. B **100**, 121109(R) (2019).

[21] M. Kiffner, J. R. Coulthard, F. Schlawin, A. Ardavan, and D. Jaksch, Manipulating quantum materials with quantum light, Phys. Rev. B **99**, 085116 (2019).

[22] S. Latini, E. Ronca, U. De Giovannini, H. Hübener, and A. Rubio, Cavity control of excitons in two-dimensional materials, Nano Lett. **19**, 3473 (2019).

[23] J. Li, D. Golez, G. Mazza, A. J. Millis, A. Georges, and M. Eckstein, Electromagnetic coupling in tight-binding models for strongly correlated light and matter, Phys. Rev. B **101**, 205140 (2020).

[24] Y. Ashida, A. İmamoğlu, J. Faist, D. Jaksch, A. Cavalleri, and E. Demler, Quantum Electrodynamic Control of Matter: Cavity-Enhanced Ferroelectric Phase Transition, Phys. Rev. X **10**, 041027 (2020).

[25] H. Gao, F. Schlawin, M. Buzzi, A. Cavalleri, and D. Jaksch, Photoinduced Electron Pairing in a Driven Cavity, Phys. Rev. Lett. **125**, 053602 (2020).

[26] F. J. Garcia-Vidal, C. Ciuti, and T. W. Ebbesen, Manipulating matter by strong coupling to vacuum fields, Science **373**, eabd0336 (2021).

[27] H. Hübener, U. De Giovannini, C. Schäfer, J. Andberger, M. Ruggenthaler, J. Faist, and A. Rubio, Engineering quantum materials with chiral optical cavities, Nat. Mater. **20**, 438 (2021).

[28] J. Li and M. Eckstein, Manipulating Intertwined Orders in Solids with Quantum Light, Phys. Rev. Lett. **125**, 217402 (2020).

[29] K. Lenk and M. Eckstein, Collective excitations of the U(1)-symmetric exciton insulator in a cavity, Phys. Rev. B **102**, 205129 (2020).

[30] A. Chiocchetta, D. Kiese, C. P. Zelle, F. Piazza, and S. Diehl, Cavity-induced quantum spin liquids, Nat. Commun. **12**, 5901 (2021).

[31] Y. Ashida, A. İmamoğlu, and E. Demler, Cavity Quantum Electrodynamics at Arbitrary Light-Matter Coupling Strengths, Phys. Rev. Lett. **126**, 153603 (2021).

[32] Z. M. Raines, A. A. Allocca, M. Hafezi, and V. M. Galitski, Cavity higgs polaritons, Phys. Rev. Res. **2**, 013143 (2020).

[33] H. Gao, F. Schlawin, and D. Jaksch, Higgs mode stabilization by photo-induced long-range interactions in a superconductor, Phys. Rev. B **104**, L140503 (2021).

[34] S. Smale, P. He, B. A. Olsen, K. G. Jackson, H. Sharum, S. Trotzky, J. Marino, A. M. Rey, and J. H. Thywissen, Observation of a transition between dynamical phases in a quantum degenerate fermi gas, Sci. Adv. **5**, eaax1568 (2019).

[35] R. J. Lewis-Swan, D. Barberena, J. R. K. Cline, D. J. Young, J. K. Thompson, and A. M. Rey, Cavity-QED Quantum Simulator of Dynamical Phases of a Bardeen-Cooper-Schrieffer Superconductor, Phys. Rev. Lett. **126**, 173601 (2021).

[36] G. S. Agarwal, R. R. Puri, and R. P. Singh, Atomic Schrödinger cat states, Phys. Rev. A **56**, 2249 (1997).

[37] F. Damanet, A. J. Daley, and J. Keeling, Atom-only descriptions of the driven-dissipative Dicke model, Phys. Rev. A **99**, 033845 (2019).

[38] S. P. Kelly, A. M. Rey, and J. Marino, Effect of Active Photons on Dynamical Frustration in Cavity QED, Phys. Rev. Lett. **126**, 133603 (2021).

[39] J. A. Muniz, D. Barberena, R. J. Lewis-Swan, D. J. Young, J. R. K. Cline, A. M. Rey, and J. K. Thompson, Exploring dynamical phase transitions with cold atoms in an optical cavity, Nature (London) **580**, 602 (2020).

[40] M. A. Norcia, R. J. Lewis-Swan, J. R. K. Cline, B. Zhu, A. M. Rey, and J. K. Thompson, Cavity-mediated collective spin-exchange interactions in a strontium superradiant laser, Science **361**, 259 (2018).

[41] R. Palacino and J. Keeling, Atom-only theories for U(1) symmetric cavity-QED models, Phys. Rev. Res. **3**, L032016 (2021).

[42] E. J. Davis, G. Bentsen, L. Homeier, T. Li, and M. H. Schleier-Smith, Photon-Mediated Spin-Exchange Dynamics of Spin-1 Atoms, Phys. Rev. Lett. **122**, 010405 (2019).

[43] A. Periwal, E. S. Cooper, P. Kunkel, J. F. Wienand, E. J. Davis, and M. Schleier-Smith, Programmable interactions and emergent geometry in an array of atom clouds, Nature **600**, 630 (2021).

[44] V. D. Vaidya, Y. Guo, R. M. Kroeze, K. E. Ballantine, A. J. Kollár, J. Keeling, and B. L. Lev, Tunable-Range, Photon-Mediated Atomic Interactions in Multimode Cavity QED, Phys. Rev. X **8**, 011002 (2018).

[45] B. P. Marsh, Y. Guo, R. M. Kroeze, S. Gopalakrishnan, S. Ganguli, J. Keeling, and B. L. Lev, Enhancing Associative Memory Recall and Storage Capacity Using Confocal Cavity QED, Phys. Rev. X **11**, 021048 (2021).

[46] K. Seetharam, A. Lerose, R. Fazio, and J. Marino, Correlation engineering via non-local dissipation, Phys. Rev. Res. **4**, 013089 (2022).

[47] J. Klinder, H. Keßler, M. Wolke, L. Mathey, and A. Hemmerich, Dynamical phase transition in the open dicke model, Proc. Natl. Acad. Sci. **112**, 3290 (2015).

[48] F. Mivehvar, F. Piazza, T. Donner, and H. Ritsch, Cavity qed with quantum gases: New paradigms in many-body physics, Adv. Phys. **70**, 1 (2021).

[49] K. Baumann, C. Guerlin, F. Brennecke, and T. Esslinger, Dicke quantum phase transition with a superfluid gas in an optical cavity, Nature (London) **464**, 1301 (2010).

[50] F. Brennecke, T. Donner, S. Ritter, T. Bourdel, M. Köhl, and T. Esslinger, Cavity qed with a bose–einstein condensate, Nature (London) **450**, 268 (2007).

[51] T. Fogarty, C. Cormick, H. Landa, V. M. Stojanović, E. Demler, and G. Morigi, Nanofriction in Cavity Quantum Electrodynamics, Phys. Rev. Lett. **115**, 233602 (2015).

[52] H. Habibian, A. Winter, S. Paganelli, H. Rieger, and G. Morigi, Bose-Glass Phases of Ultracold Atoms due to Cavity Backaction, Phys. Rev. Lett. **110**, 075304 (2013).

[53] L. Himbert, C. Cormick, R. Kraus, S. Sharma, and G. Morigi, Mean-field phase diagram of the extended Bose-Hubbard model of many-body cavity quantum electrodynamics, Phys. Rev. A **99**, 043633 (2019).

[54] T. Keller, V. Torggler, S. B. Jäger, S. Schütz, H. Ritsch, and G. Morigi, Quenches across the self-organization transition in multimode cavities, New J. Phys. **20**, 025004 (2018).

[55] T. Keller, S. B. Jäger, and G. Morigi, Phases of cold atoms interacting via photon-mediated long-range forces, J. Stat. Mech.: Theory Exp. (2017) 064002.

[56] S. Schütz, S. B. Jäger, and G. Morigi, Dissipation-Assisted Prethermalization in Long-Range Interacting Atomic Ensembles, Phys. Rev. Lett. **117**, 083001 (2016).

[57] M. Xu, S. B. Jäger, S. Schütz, J. Cooper, G. Morigi, and M. J. Holland, Supercooling of Atoms in an Optical Resonator, Phys. Rev. Lett. **116**, 153002 (2016).

[58] E. A. Yuzbashyan, M. Dzero, V. Gurarie, and M. S. Foster, Quantum quench phase diagrams of an s-wave BCS-BEC condensate, Phys. Rev. A **91**, 033628 (2015).

[59] J. Dukelsky, S. Pittel, and G. Sierra, Colloquium: Exactly solvable Richardson-Gaudin models for many-body quantum systems, Rev. Mod. Phys. **76**, 643 (2004).

[60] R. W. Richardson, New Class of Solvable and Integrable Many-Body Models, arXiv:cond-mat/0203512.

[61] R. A. Barankov and L. S. Levitov, Synchronization in the BCS Pairing Dynamics as a Critical Phenomenon, Phys. Rev. Lett. **96**, 230403 (2006).

[62] R. A. Barankov, L. S. Levitov, and B. Z. Spivak, Collective Rabi Oscillations and Solitons in a Time-Dependent BCS Pairing Problem, Phys. Rev. Lett. **93**, 160401 (2004).

[63] E. A. Yuzbashyan, B. L. Altshuler, V. B. Kuznetsov, and V. Z. Enolskii, Nonequilibrium Cooper pairing in the nonadiabatic regime, Phys. Rev. B **72**, 220503(R) (2005).

[64] E. A. Yuzbashyan, B. L. Altshuler, V. B. Kuznetsov, and V. Z. Enolskii, Solution for the dynamics of the BCS and central spin problems, J. Phys. A: Math. Gen. **38**, 7831 (2005).

[65] E. A. Yuzbashyan, O. Tsyplyatyev, and B. L. Altshuler, Relaxation and Persistent Oscillations of the Order Parameter in Fermionic Condensates, Phys. Rev. Lett. **96**, 097005 (2006).

[66] M. A. Norcia and J. K. Thompson, Cold-Strontium Laser in the Superradiant Crossover Regime, Phys. Rev. X **6**, 011025 (2016).

[67] See Supplemental Material at http://link.aps.org/supplemental/10.1103/PhysRevResearch.4.L042032 for a discussion of the band structure and equilibrium phase diagram.

[68] P. Kirton and J. Keeling, Suppressing and Restoring the Dicke Superradiance Transition by Dephasing and Decay, Phys. Rev. Lett. **118**, 123602 (2017).

[69] P. Kirton and J. Keeling, Superradiant and lasing states in driven-dissipative Dicke models, New J. Phys. **20**, 015009 (2018).

[70] P. Kirton, M. M. Roses, J. Keeling, and E. G. D. Torre, Introduction to the Dicke Model: From Equilibrium to Nonequilibrium, and Vice Versa, Adv. Quantum Technol. **2**, 1800043 (2019).

[71] R. W. Richardson and N. Sherman, Exact eigenstates of the pairing-force hamiltonian, Nucl. Phys. **52**, 221 (1964).

[72] M. Gaudin, Diagonalisation d'une classe d'hamiltoniens de spin, Journal de Physique **37**, 1087 (1976).

[73] See SM for details on Lax Analysis.

[74] See SM for details on mean field approximation for Lindblad Evolution.

[75] See SM for the relation between resonance and minimum of photon density.

[76] C. D. Bruzewicz, J. Chiaverini, R. McConnell, and J. M. Sage, Trapped-ion quantum computing: Progress and challenges, Appl. Phys. Rev. **6**, 021314 (2019).

[77] D. E. Chang, J. S. Douglas, A. González-Tudela, C.-L. Hung, and H. J. Kimble, Colloquium: Quantum matter built from nanoscopic lattices of atoms and photons, Rev. Mod. Phys. **90**, 031002 (2018).